19th Australasian Tunnelling Conference – Acosta-Martínez, Stewart and Hudson-Smith (Eds.)

Towards reliable UCS inputs for tunnel design: Learnings from Snowy 2.0

A. Chen & M. Zoorabadi
SMEC, Australia

K. Stariha
Snowy Hydro Limited, Australia

ABSTRACT: UCS is a critical parameter in underground tunnel design, serving as a fundamental input for numerical modelling. However, current practices in tunnel design often face challenges due to reliance on UCS results obtained during the geotechnical investigation stage, where limited borehole coverage may lead to a biased estimation. Variations in UCS results across laboratories can introduce inconsistencies due to differences in apparatus, interpretation methods and descriptions of failure mode. This paper addresses these gaps by leveraging the extensive UCS testing conducted for Snowy 2.0 project, particularly in its power station caverns. The project not only incorporated a wide range of UCS but also executed a proficiency test across labs using identically prepared grout samples. The study features a statistical analysis, a failure type screening and a discussion of using UCS in Hoek-Brown's criterion. This work underscores the importance of UCS data processing and its critical role in bridging gaps in current geotechnical practices

1 INTRODUCTION

Uniaxial Compressive Strength (UCS) and Young's Modulus (E) are fundamental parameters in the design and construction of underground works. UCS provides a direct measure of the peak compressive strength of intact rock under unconfined conditions, while E quantifies the elastic stiffness of the rock, governing its deformation response under applied stress. Accurate determination of both parameters is essential for numerical modeling, support design, and predicting ground behavior during and after excavation. Although there are other more advanced laboratory and in-situ tests available for characterizing rock strength and deformation properties, the UCS test remains widely used in the industry due to its simplicity and cost-effectiveness. Both UCS and E can be derived from a single test procedure, making it highly efficient in terms of sample usage and testing time. The straightforward setup and minimal equipment requirements, make the test a practical choice for site investigations, however there are limitations inherent in the test process itself which are not always accounted for in practice. Geological variability, laboratory practices, and data interpretation methods can significantly affect the derived inputs. This paper will utilize the UCS test data obtained from the geotechnical investigations conducted as part of the Snowy 2.0 project. The extensive database from this large-scale infrastructure development provides a valuable opportunity to examine the reliability, variability, and practical interpretation of UCS and E modulus results in the context of real-world engineering applications. The study will focus on UCS and E as design inputs only and will not comment further on other inputs for rock mass strength estimation.

2 PROJECT OVERVIEW AND SCOPE OF THE STUDY

Snowy 2.0 is a major pumped hydro expansion of the Snowy Mountains Hydroelectric Scheme in New South Wales, Australia, aimed at providing large-scale energy storage and grid stability to support the nation's transition to renewable energy. The Power Station Complex (PSC) is a major feature of Snowy 2.0, consisting of a Machine Hall and a Transformer Hall, with a maximum span of 33m and overburden of 600-750m (Figure 1).

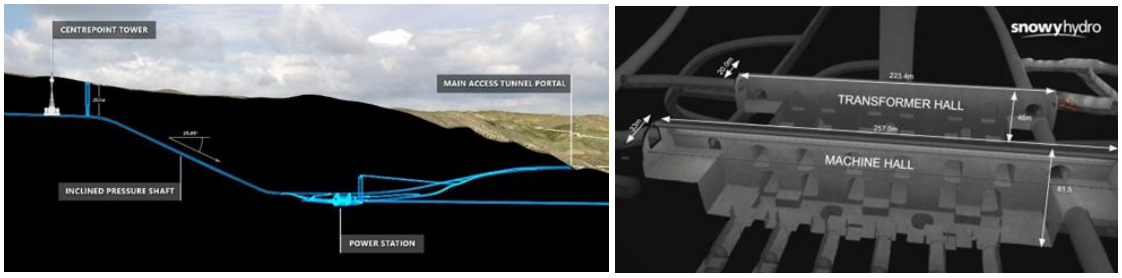

Figure 1. General location and layout of the PSC.

A total of 247 UCS test results were compiled, incorporating data from cored holes undertaken both pre-construction from the surface and during construction, into the PSC area from adjacent construction tunnels (Figure 2). The majority of UCS tests were performed in accordance with AS 4133.4.3.1 and AS 4133.4.3.2, which also outline deformability-related parameters such as Secant (E_s) and Tangent (E_t) Young's Modulus and Poisson's Ratio (v). Results have been used to inform the intact rock strength during the design phase, as well as to support design verification throughout the construction phase. This study will focus on the examination of the two principal parameters derived from this testing - UCS and E_s values of 69.1 MPa and 45.1 GPa respectively, with standard deviations of 35.7 MPa and 13.2 GPa.

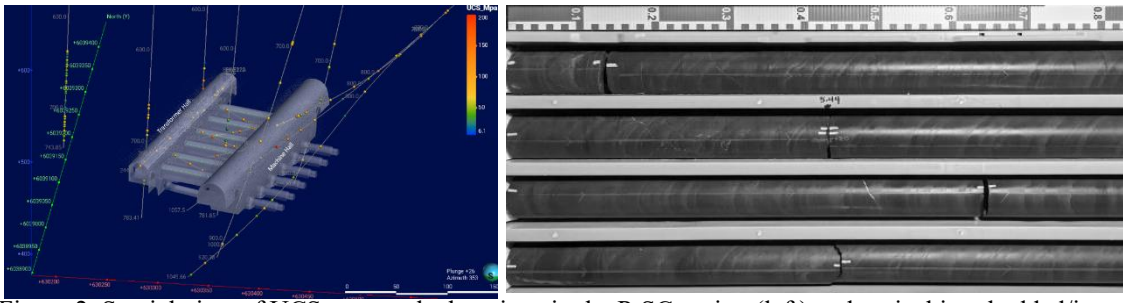
Figure 2. Spatial view of UCS test results locations in the P SC region (left) and typical interbedded/interlaminated sandstone & siltstone in RBW formation (Right).

The PSC area is set in the Silurian age Ravine Bed West Formation (RBW), which comprises interbedded to interlaminated metasiltstone and metasandstone, with minor conglomerate. Due to the involvement of several laboratories over a period of 7 years, the lithological descriptions and break types recorded during UCS testing were not consistent across all datasets. To address this, the project owner's geology team re-assessed the lithology and break types of all tested samples, ensuring greater consistency and accuracy in classification. As a result of the re-assessment of lithology, the 247 samples were classified as follows: 233 samples as interbedded or interlaminated sandstone and siltstone, 6 samples as conglomerate, 5 samples as interbedded conglomerate and sandstone, and 3 samples as sandstone. Since the influence of grain size variation in sedimentary rocks on UCS and E_s is well documented/ and observed (UCS for 3 sandstone samples vary from 182-270 MPa, significantly larger than global mean), and most of the samples (233 out of 247) are classified as interbedded or interlaminated sandstone and siltstone, the subject of this study is limited to this lithological group.

3 ASSESSMENT OF FAILURE MODE ON UCS AND YOUNG'S MODULUS

3.1 *Re-assessment of failure mode: Intact vs Discontinuity-controlled*

An overview of the data and laboratory reports indicates that both UCS and E_s exhibit high variability. In addition, many samples show failure modes influenced by natural defects, suggesting that these results are not fully representative of intact rock properties. Variations in failure mode descriptions, even within the same laboratory, further complicate the differentiation between intact and discontinuity-controlled failures. To address this, the owner's engineering team re-assessed the failure modes using a project-specific guideline developed based on the work of Basu et al. (2013) and Chakraboty et al (2019). The failure mode classifications are summarized in Table 1, along with a pie chart illustrating the distribution following re-assessment. Representative core samples for each typical failure mode are presented in Figure 3. Spalling failure mode is excluded from assessment since it is considered as a premature and therefore invalid mode.

The distributions of UCS and E_s are presented in Figure 4, showing both histograms categorized by failure mode and normalized probability distribution curves. Key statistical results are summarized in Table 2. For UCS, samples exhibiting Joint/Vein failure modes display significantly lower strength, with a mean value of 37.7 MPa compared to the overall mean of 65.8 MPa. In contrast, samples with Shattered failure modes show substantially higher UCS values, with a mean of 100.2 MPa. Other failure types exhibit mean UCS values relatively close to the global mean. A similar trend is observed for E_s; however, the variance between failure modes is considerably smaller, suggesting that E_s is less sensitive to failure mode differences compared to UCS.

Table 1. Failure modes and description assigned by Owner's Engineering team

	Description	Summary
Shear	Break along single or multiple shear plane	Intact rock failure
Split	Axial splitting / Tensile dominated	Intact rock failure
Shatter	Shattered	Intact rock failure
Bedding	Break along foliation, bedding or cleavage	Discontinuity induced failure
Joint/Vein	Break along natural defect (joint, vein)	Discontinuity induced failure
Mixed mode	Break along multiple axial planes	Combination of intact and discontinuity failure
Spall	Minor break	Intact rock failure (premature, invalid)

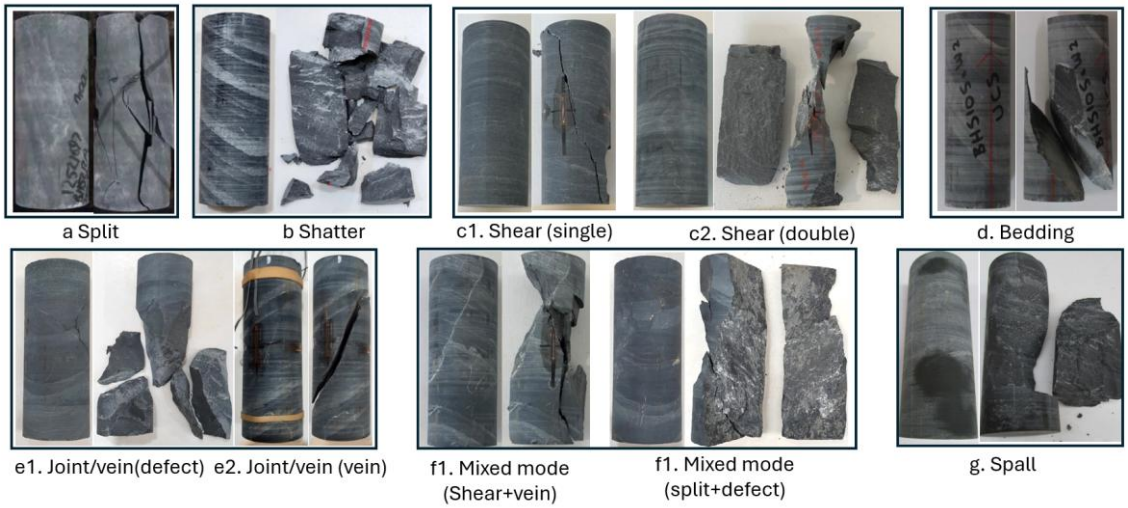

Figure 3. Examples of typical assigned failure modes, with samples before test at the left.

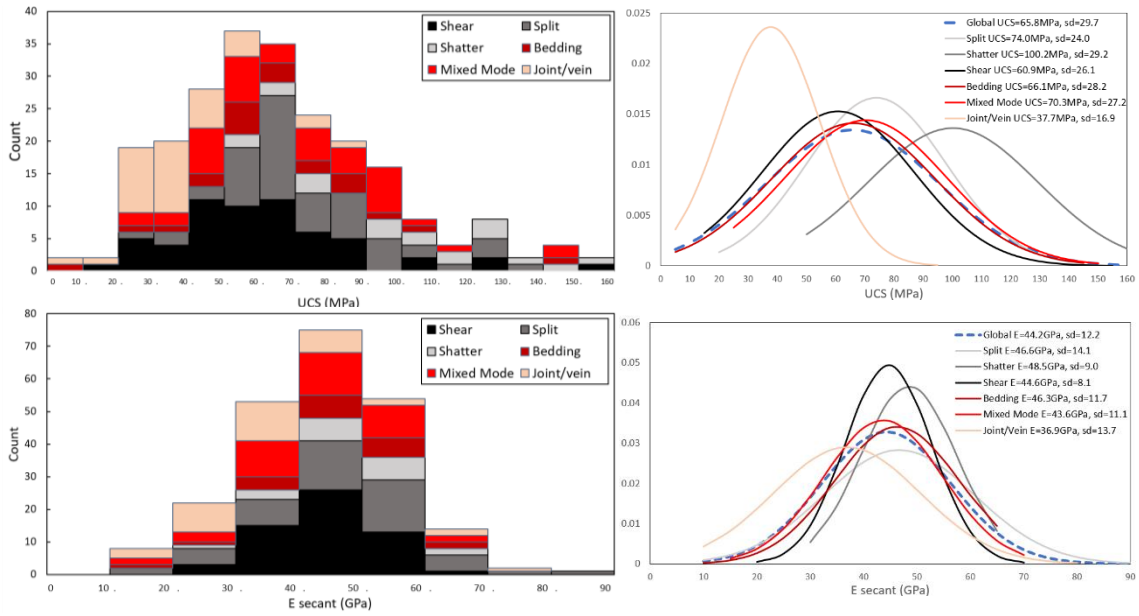

Figure 4. UCS (top) and E_s (bottom) distribution for different failure modes, presented by histogram (left) and normalized probability curve (right).

Table 2. Summary of statistical analysis results for UCS and E_s with different failure modes

		UCS			E_s		
Failure Mode	Count	Mean	Median	Mode	Mean	Median	Mode
Split	55	74.0	68.4	60-70	46.6	48.8	50-60
Shatter	20	100.2	100.2	N.A.*	48.5	48.9	40-50,50-60
Shear	58	60.9	58.4	50-60	44.6	45.8	40-50
Bedding	21	66.1	64.5	50-60	46.3	47.9	40-50
Mixed Mode	41	70.3	66.4	N.A.*	43.6	45.4	40-50
Joint/Vein	36	37.7	33.2	30-40	36.9	35.6	40-40
Global	233	65.8	64.4	50-60	44.2	64.4	40-50

*Modes for Shatter and Mixed mode is not defined due to 3 or more bins with the same count, which also indicates the UCS for these two are non-normally distributed. Refer to Histogram in Figure 4 for explicit data.

It should be noted that, as the reassessment relied primarily on photographs provided in laboratory reports (which were often unclear), substantial weight was still placed on the original laboratory descriptions. Additionally, the term "Mixed Mode" can be ambiguous when differentiating between intact and discontinuity-controlled failures: while some Mixed Mode cases involve combinations of intact failure mechanisms, others clearly involve discontinuity-driven behaviour. This mixed nature also explains why the average UCS and E_s values for Mixed Mode samples are relatively close to the global mean, reflecting the contribution of both stronger intact failures and weaker discontinuity-controlled failures within this group. To maintain a conservative approach, for this study all Mixed Mode failures were classified as discontinuity controlled.

3.2 *Further discussion on Veins and Beddings controlled failure*

In the failure modes described in 3.1, “Joint/Vein” failure mode is assigned if a failure plane occurs along visible surface veins. Within the RBW formation, veins are often present (Figure 2 and Figure 3), however the nature of veins varies in orientation (random or parallel with bedding), aperture and mineralogy – all of which may affect the UCS. Furthermore, micro-veins may be present which are not easily visible. This may trigger initial cracking at a lower strength, mislabeling the failure type to intact modes. The influence of veins on UCS has been discussed extensively in the literature (Everall 2019, Martin 2022, Rudderham 2023, Wang 2025), the author does not intend to elaborate further but wishes to emphasize the importance of identifying and

recording vein features during construction, as they can have a significant impact on the assessment of intact rock strength.

The "Bedding" failure mode (occurring along sandstone–siltstone bedding / laminations) presents similar challenges. Only a small proportion of samples failed in this mode. Both very low and very high UCS results were observed within this category, and in some cases intact failures had lower results than bedding failures. The impact of bedding on UCS has been studied by researchers like Davarpanah et al (2020), however as this topic involves complex geological and mechanical interactions, the author does not intend to elaborate further but notes its significance for interpretation.

4 EFFECTS FROM LABORATORY PRACTICES FACTORS

While analysing the data, the owner's engineering team observed that laboratory practices themselves may contribute to variation within the dataset. To further investigate this, a "proficiency test" was conducted. Theoretically identical grout specimens were sent to five laboratories 4 contracted to Snowy 2.0 and one external, labelled A, B, C, D, E. Each laboratory tested three samples followed the procedures outlined in AS 4133.4.3.2, while one (Lab E) followed the ISRM Suggested Methods. Unlike typical laboratory reporting, raw data files were also made available for independent interpretation by the engineering team. The key results of the proficiency test are summarized in Table 3, along with stress–strain curves re-generated from the raw data.

Table 3. Key results from the internal proficiency tests, with max. & min. values underlined.

LAB	ID	UCS (MPa)	E_s (GPa)	v	Failure Mode	Stress vs Strain plot
A	A1	38.0	28	0.27	shear	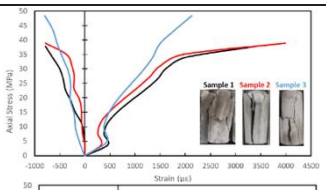
	A2	39.0	30	0.18	shear	
	A3	48.0	25	0.29	shear+split	
B	B1	42.8	23.3	0.06	shear+split	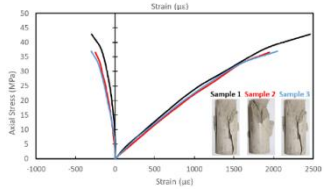
	B2	36.6	22.2	0.10	shear	
	B3	37.0	22.5	0.11	shear	
C	C1	39.0	24	0.05	split	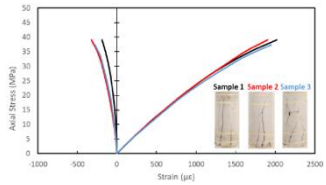
	C2	39.0	24	0.12	shear+split	
	C3	37.0	24	0.10	shear+split	
D	D1	38.9	23.2	0.20	spalling	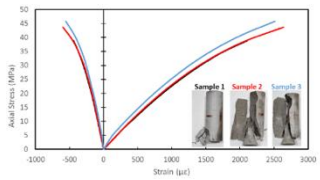
	D2	43.6	23.3	0.20	shear	
	D3	45.7	24.5	0.20	shear	
E	E1	49.7	24.1	0.16	split	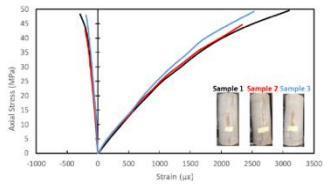
	E2	44.7	25	0.13	split	
	E3	49.3	23.7	0.12	split	

Despite the use of theoretically identical specimens and four (A, B, C, D) laboratories following the same AS 4133.4.3.2 standard, noticeable variation is observed. UCS values range from 36.6 MPa to 48 MPa, showing a spread of around ±15%, while E_s values are more consistent, clustering between 22 GPa and 30 GPa. Failure mode classification shows greater inconsistency. For Lab A, a constant loading rate was not achieved, making its higher E_s questionable. The variation observed, even under common testing standards, highlights that laboratory practice and control (rather than methodology differences) are key contributors to data variability, emphasizing the need for stricter procedural enforcement to ensure reliable results.

4.1 *Further discussion on effects of loading rate*

For the proficiency test described above, Laboratory E followed ISRM Suggested Methods rather than AS 4133.4.3.2. The primary difference between the two standards lies in the loading rate requirements: AS 4133.4.3.2 specifies a displacement rate of ≤ 0.1 mm/min, whereas ISRM requires a constant stress rate of 0.5–1.0 MPa/s. This difference appeared to directly contribute to higher UCS results for Laboratory E. To further investigate this effect, graphs of loading rate and test duration versus UCS have been plotted in Figure 5, using both the proficiency test data and the Snowy 2.0 PSC SI sample results. Clear correlations between loading rate, test duration, and UCS are evident. No such trend was observed for E_s; therefore, it is not presented.

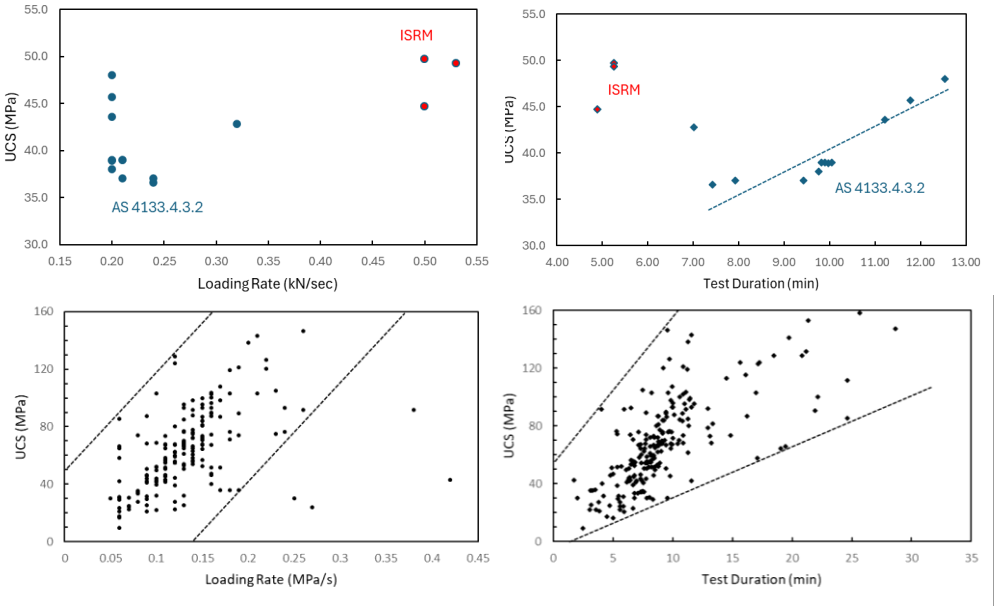

Figure 5. Plots of Loading Rate (left) and Test Duration against UCS. Results from top are from the proficiency test and bottom are from Snowy 2.0's site investigation UCS tests.

The effect of loading rate on UCS is a well-known and extensively discussed topic, encompassing aspects such as ductile versus brittle behavior, energy dissipation mechanisms, strain rate sensitivity, and crack propagation dynamics (Cao 2019, Závacký 2019). As these discussions are highly scientific and outside the intended scope of this study, the author instead highlights two key practical observations: (1) Loading rate requirements vary significantly across different codes and standards, as shown in Table 4. The bias introduced by different loading controls can be substantial. For example, in the Snowy 2.0 PSC dataset, all tests with recorded loading rates were below 0.4 MPa/s, which is below the minimum specified in EN 1926:2006 and the ISRM Suggested Methods (2) Among the standards considered, AS 4133 is the only one that differentiates loading rate requirements based on rock strength. While this appears to be a reasonable approach, it has introduced complications where the sample strength is close to the boundary between methods. E.g., in the Snowy 2.0 PSC dataset 29% of samples lie between 40-60 MPa. This raises the

question of whether the appropriate standard procedures were consistently applied for UCS values in these cases.

Table 4. Requirement on loading rates from different standards & codes

Standard	Loading Rate Requirement
AS 4133.4.3.1:2009 (UCS ≥ 50 MPa)	Load continuously at a constant stress rate so that failure occurs within 5–15 minutes.
AS 4133.4.3.2:2022 (UCS < 50 MPa)	Load continuously without shock; achieve a displacement rate ≤ 0.1 mm/min.
EN 1926:2006 (2006)	Load continuously at a constant stress rate of (1 ± 0.5) MPa/s.
ASTM D2938-95 (2017)	Load continuously without shock. Maintain a constant stress or strain rate to produce failure between 2–15 minutes. Stress/strain rate must not deviate by more than ±10%.
ISRM Suggested Methods (2018)	Load continuously at a constant stress rate of 0.5–1.0 MPa/s, aiming for failure within 5–10 minutes.

5 DISSCUSSION ON USING OF UCS RESULTS IN HOEK-BROWN CRITERION

In rock-mass parameter interpretation, the GSI–Hoek-Brown system is typically combined with the Hoek–Diederichs modulus equation to build the constitutive model. The Hoek-Brown formulation treats the intact unconfined compressive strength (σ_{ci}) and intact material constant (m_i) as baseline inputs that are subsequently reduced by GSI and disturbance factors to give rock-mass parameters. Hoek & Brown (1968, 1983, 2018, 2023) have consistently highlighted the preference for triaxial testing over UCS testing in the derivation of σ_{ci}, noting that many UCS specimens fail by axial splitting or mixed tensile mechanisms, whereas the criterion is intended to describe shear failure. Bewick et al. (2015, 2019) likewise advise excluding UCS results from σ_{ci} determination unless failure-mode screening is performed to include only specimens that show a clear shear break. Snowy 2.0 PSC samples were tested with a complete, high-quality triaxial programme that satisfies the original Hoek (1983) requirements σ_{ci} has been derived directly from triaxial data using the recommended regression procedure (Table 5). The derived σ_{ci} is 97.5 MPa, significantly larger than the global UCS (65.8 MPa) and the suggested shear-mode failure UCS (60.9 MPa), but interestingly close to the shatter-mode failure UCS (100.2 MPa). This warrants additional investigation together with the consideration of effects from loading rates & microstructures, as discussed earlier.

Table 5. σ_{ci} and m_i from Snowy 2.0 triaxial results, calculated following Hoek (1983).

Test ID	Rupture angle	R^2	σ_{ci} (MPa)	*mi*
1a	75	0.96	59.9	5.08
1b	70	0.88	97.3	5.64
2a	50	0.99	104	7.15
2b	60	0.99	98.2	8.13
4a	45	0.90	99.8	6.65
4b	60	0.96	119	9.37
5a	70	0.94	89.1	7.74
5b	70	0.98	112	7.54
Mean	62.5	0.95	97.5	7.16

6 CONCLUSION AND RECOMMENDATION

This paper investigated the processing and reliability of UCS data based on the extensive Snowy 2.0 database. A project-specific re-assessment of lithology and failure modes significantly enhanced the clarity of the dataset and demonstrated the value of targeted re-screening in improving

the interpretation of UCS. Two key sources of variability were identified: (i) laboratory practices, and (ii) the broad and often loosely defined loading-rate requirements across existing standards, particularly the impracticality of the 50 MPa boundary specified in the AS 4133.4.3.1 and AS 4133.4.3.2. Noting the difficulties in such a task, an industry-wide discussion is recommended on the specification of loading rates in testing standards. Alternately, major projects could consider adopting a project-specific loading-rate specification after achieving a good understanding of the fundamental geotechnical conditions. It is worth highlighting the importance of supervising, reviewing, and providing feedback to laboratories to ensure the ongoing reliability of test results. Additionally, comparison between UCS-derived inputs and industry-standard Hoek-Brown rock mass estimation methods revealed that UCS results tended to underestimate the intact compressive strength (σ_{ci}) relative to triaxial regression. These findings highlight the importance of a rigorous, site-specific approach to selecting design parameters for numerical modelling and empirical assessments.

Snowy 2.0's unusually large, fully documented dataset offers a rare benchmark for deeper study of loading-rate effects, laboratory reproducibility and intact-to-rock-mass conversions. Continued scientific analysis of this material is strongly encouraged to refine test standards and to anchor empirical design methods in more defensible, project-specific evidence.

7 REFERENCES

ASTM International (2017). ASTM D2938–95: Standard Test Method for Unconfined Compressive Strength of Intact Rock Core Specimens.

Basu A, Mishra A, Roychowdhury K (2013) Rock failure mode sunder uniaxial compression, Brazilian, and point load tests. Bull Eng Geol Environ 72:457–475.

Bewick, R. P.et al. (2015). Interpretation of UCS Test Results for Engineering Design. Proceedings 13th International Congress of Rock Mechanics - ISRM Congress 2015, Montreal, 1-14.

Bewick, R. P.et al. (2019). Strength of massive to moderately jointed hard rock masses. Journal of Rock Mechanics and Geotechnical Engineering, 11, 562-575.

Cao, S. et al. (2019). Loading rate effect on uniaxial compressive strength behavior and acoustic emission properties of cemented tailings backfill. *Construction and Building Materials* 213 (2019) 313–324.

Chakraboty, S. et al (2019). Failure Modes of Rocks under Uniaxial Compression Tests: An Experimental Approach. Volume 2, Issue 3. Journal of Advances in Geotechnical Engineering.

Davarpanah, S.M. et al. (2020). Technical Note: Determination of Young's Modulus and Poisson's Ratio for Intact Stratified Rocks and their Relationship with Uniaxial Compressive Strength. *AUSTRALIAN GEOMECHANICS VOLUME* 55: NO.4.

European Committee for Standardization (CEN) (2006). EN 1926:2006: Natural Stone Test Methods – Determination of Uniaxial Compressive Strength.

Everall, T.J. et al. (2018) The Influence of Pre-Existing Deformation and Alteration Textures on Rock Strength, Failure Modes and Shear Strength Parameters. *Geosciences* 2018, 8(4), 124.

Hoek, E (1968). Brittle Fracture of Rock. Rock Mechanics in Engineering Practice.

Hoek, E (1983). Strength of jointed rock masses. Lecture notes. Geotechnique, Vol.23, No.3, 1983, pp. 187-223.

Hoek, E & Brown, E.T (2019). The Hoek-Brown failure criterion; and GSI – 2018 edition. Journal of Rock Mechanics and Geotechnical Engineering 11 (2019) pp. 445-463.

Hoek, E. (2023). *Practical Rock Engineering*, Chapter 3: Intact Rock Strength. Toronto: Rocscience Inc., 34 pp. Available at: https://www.rocscience.com/learning/practical-rock-engineering.

International Society for Rock Mechanics (ISRM) (2018). Suggested Methods for Determining the Uniaxial Compressive Strength and Deformability of Rock Materials.

Martin, L et al. (2022). Relationship between fissility, composition, rock fabric and reservoir properties in Vaca Muerta Formation (Neuquén Basin, Argentina): from outcrop to subsurface core data. *Andean Geology* 49(3).

Rudderham, G.A. & Day, J.J. (2023). Veined Rock Performance under Uniaxial and Triaxial Compression Using Calibrated Finite Element Numerical Models. *Geotechnics* 2023, 3(4), 1219-1250.

Standards Australia (2009). AS 4133.4.3.1–2009: Method 4.3.1: Rock Strength Tests – Determination of Deformability of Rock Materials in Uniaxial Compression – Strengths of 50 MPa and Greater.

Standards Australia (2022). AS 4133.4.3.2–2022: Method 4.3.2: Rock Strength Tests – Determination of the Deformability of Rock Materials and Uniaxial Compressive Strength – Rock Strength Less Than 50 MPa.

Wang, H. et al. (2025). An Investigation of the Effect of Fissure Inclination on Specimen Deformation and the Damage Mechanism Based on the DIC Method. Buildings 2025, 15, 71.

Závacký, M & Stefanak, J (2019). Strains of Rock During Uniaxial Compression Test. Article No. 32, The Civil Engineering Journal 3-2019.